

Aging by near-extinctions in many-variable interacting populations

Thibaut Arnoulx de Pirey and Guy Bunin

Department of Physics, Technion-Israel Institute of Technology, Haifa 32000, Israel

The dynamics of multiple interacting populations feature extinctions, meaning that zero population size is an absorbing value of the dynamics. In certain few-variable systems, this can lead to attracting sets along which the dynamics slow down by moving ever closer to unstable fixed points. Recently, there has been evidence of related effects in many-variable dynamics. Here, we investigate the connection between extinction and dynamical slowdown (aging) by introducing an exactly solvable many-variable model with two absorbing values per degree of freedom. We show that aging emerges generically when random interactions are taken between populations. The mechanism for aging is different from the one at play in usual glassy systems: For most of the time, variables are exponentially close (in time) to absorbing values with rapid transitions between them, resulting in long sojourn times near unstable fixed points.

The dynamics of populations that interact and reproduce, as in ecosystems harboring different species, are often modeled by coupled ordinary differential equations for population sizes $\{x_i\}$. They are non-negative variables, $x_i \geq 0$, and must remain so throughout the dynamics. The boundary values $x_i(t) = 0$ represent extinct populations: if a population is extinct at some time t , it must remain so at all later times. Namely, $x_i = 0$ is an absorbing value for x_i . These requirements are satisfied by a broad class of differential equations of the form [1]

$$\dot{x}_i = x_i g_i(\vec{x}). \quad (1)$$

Examples in this class include the Lotka-Volterra equations for which $g_i(\vec{x}) = B_i - \sum_j A_{ij} x_j$, with the matrix \mathbf{A} encoding the interactions between populations; resource-competition models [2]; and the replicator equations employed in evolution and game theory [1].

It is well-known that, depending on the shape of the functions g_i , few variable systems of the form (1) can exhibit different long-time behaviors such as stationarity, periodicity or chaos [1]. Remarkably, the existence of absorbing hyperplanes has also been shown to lead, in some cases, to robust heteroclinic cycles [3, 4]. A classical example is the three-species Lotka-Volterra system with rock-paper-scissors type interactions [5], where each species hinders the growth of the next. There, trajectories are attracted to a cycle connecting three unstable fixed points, each with a single surviving population, see Fig. 1(a). As time increases, they pass ever closer to these fixed points, resulting in slowdown of the dynamics, with exponentially increasing sojourn times in their vicinity and rapid transitions between them [5, 6].

In systems characterized by a large number S of variables, recent works find that an analogous slowdown emerges generically for random interaction coefficients. It is known that aging (a situation in which the system does not asymptotically settle to a fixed point but keeps exploring the phase space with a velocity that nevertheless decays with the elapsed time) can occur in many-variable

Lotka-Volterra systems [7] with random asymmetric interactions and replicator equations [8] with nearly anti-symmetric random interactions. Here, some populations experience ever longer periods near extinction ($x_i \simeq 0$ and x_i closer to zero in successive near-extinction periods) before eventually returning to $x_i = O(1)$, see Fig. 1(b). Such dips are of ecological significance, as they may lead to extinctions in actual finite populations. The properties of these dynamics have remained elusive, however. The analogy with low-dimensional examples such as in Fig. 1(a) is limited. For one, in the many-variable case, the system does not approach a limit-cycle (at least if the limit $S \rightarrow \infty$ is taken before $t \rightarrow \infty$). Secondly, large dynamical systems of the form (1) may possess many fixed points with different properties (e.g., the fraction of variables for which $x_i = 0$ or their instability index), and linking the characteristics of fixed points to the dynamics remains an open problem. In this work, we propose a high-dimensional model of the form (1) that provides insights into the connection between aging and absorbing values, by bypassing some of the difficulties inherent to the many-variable Lotka-Volterra and replicator equations. Fixed points of (1) satisfy either $x_i = 0$ or $g_i(\vec{x}) = 0$ for every i . Since the unique aging behavior of these systems is tied to the existence of absorbing values ($x_i = 0$), we introduce a model with *two* absorbing values for each variable, which we refer to as the mirrored-extinction model. Specifically, we consider the evolution of S degrees of freedom $\{x_i\}_{i=1,\dots,S}$, with $0 \leq x_i \leq 1$ for all i ,

$$\dot{x}_i(t) = x_i(t) \left[1 - x_i(t) \sum_{j=1}^S \alpha_{ij} x_j(t) \right], \quad (2)$$

where α is a zero-mean Gaussian random matrix with variances $\mathbb{E}[\alpha_{ij}\alpha_{mn}] = \delta_{im}\delta_{jn}/S$. The resulting dynamical system has many fixed points where all degrees of freedom are at their absorbing values, either $x_i = 0$ or $x_i = 1$, allowing us to focus on the effects of these absorbing boundaries. Importantly, the model in (2) is exactly

solvable in high dimension, allowing us to obtain detailed information and deeper insight on this family of systems. It displays aging, similarly to the Lotka-Volterra case, but with the x_i spending ever longer times close to either $x_i = 0$ or 1 with rapid transitions between these two values, see Fig. 1(b). From an ecological perspective, the interactions in (2) affect the growth-rates of populations but not their maximal size, which might be limited by other factors, see for example [9, 10].

The mechanism for aging found here is drastically different from that at play in aging of usual spin-glasses following a quench, where the system's energy is reduced until it reaches an energy surface dominated by marginally-stable fixed points and spends its time there [11–13]. This includes Lotka-Volterra dynamics with *symmetric* interaction matrices α_{ij} [14, 15], where $\vec{g}(\vec{x})$ is the gradient of a potential, thus permitting a mapping to a spin-glass phase. This form of aging is known to disappear when asymmetry is introduced to the interaction coefficients [16, 17].

In contrast, here we show that aging happens in (2), as variables are driven close to their absorbing values, where their dynamics slow down. Similarly to the three-variable example of Fig. 1(a), typical systems go very close to fixed points which are therefore long-lived, see Fig. 1(b,c), despite being *unstable*. This provides a mechanism for aging in the absence of an underlying energy function. We find that, in the long-time limit, the system moves between infinitely many unstable fixed points that all have the same finite fraction of unstable directions and the same stability spectrum. They are neither the most stable nor the most abundant fixed points.

Dynamical mean field theory—To analyze the many-variable dynamics (2), we use dynamical mean field theory (DMFT) [18, 19]. In the limit $S \rightarrow \infty$ and for x_i sampled independently at the initial time, the dynamics of a single degree of freedom $x(t)$ are exactly described by a stochastic differential equation

$$\dot{x}(t) = x(t) [1 - x(t)] \xi(t), \quad (3)$$

with $\xi(t)$ a zero mean Gaussian process. This stems from the fact that the term $\xi_i(t) \equiv \sum_j \alpha_{ij} x_j(t)$ appearing in (2) is the sum of many weakly correlated contributions. As is usual in DMFT, this expression for $\xi_i(t)$ yields a self-consistent closure relation that reads $C(t, t') \equiv \langle \xi(t) \xi(t') \rangle = \langle x(t) x(t') \rangle$. Here the angular brackets $\langle \cdot \rangle$ denote an average over the initial conditions $x(0)$ and realizations of the noise $\xi(t)$. The derivation of (3) follows a standard procedure [7, 18–21] and is detailed in App. I. To analyze the dynamics, it is therefore crucial to solve for the autocorrelation function $C(t, t')$.

To proceed, we introduce the transformation $u(t) = \ln[x(t)/(1-x(t))]$ that sends the boundaries of the domain $[0, 1]$ to $(-\infty, +\infty)$ and for which (3) becomes

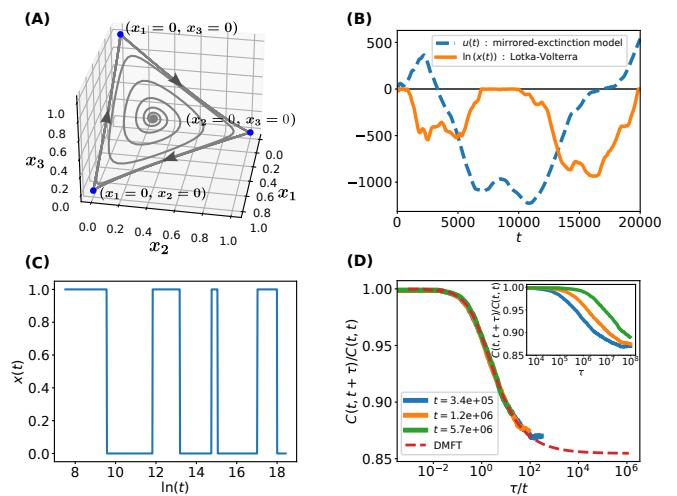


Figure 1. **Aging by passing near unstable fixed points.** (A) Heteroclinic cycle in the three-variable May-Leonard model. The dynamics slow down as the system goes ever closer to fixed points (dots), despite them being unstable. (B) Dynamics of example variables (out of $S = 2 \cdot 10^4$), in the Lotka-Volterra system (solid line, plot of $\ln x_i$) and the mirrored-extinction model (2), (dashed, plot of $\ln[x_i/(1-x_i)]$). This illustrates the longer and deeper excursions near the absorbing values, $x_i = 0$ for Lotka-Volterra and $x_i \in \{0, 1\}$ for the mirrored-extinction case. (C) In log-time, the dynamics of any variable in (2) eventually follow a biased time-translation invariant two-state process. (D) Mean autocorrelation function $C(t' + \tau, t')$ of $x_i(t)$ as measured in a numerical simulation of (2) with $2 \cdot 10^4$ degrees of freedom as a function of τ/t' , showing a collapse for different waiting times t' , and agreement with the analytical master curve (dashed line). Inset: same curves, as a function of τ . Parameters for Lotka-Volterra simulations in (A,B) are given in App. II.

$$\dot{u}(t) = \xi(t), \quad (4)$$

with the closure relation

$$\langle \xi(t) \xi(t') \rangle = \langle f(u(t)) f(u(t')) \rangle, \quad (5)$$

where

$$f(y) \equiv \frac{e^y}{1 + e^y}.$$

Aging and the auto-correlation function—We start by showing that the mean-square displacement of $u(t)$ is ballistic. Denote the auto-correlation $G(t, t') \equiv \langle u(t) u(t') \rangle$, which by (4) is related to $C(t, t')$ by $C(t, t') = \partial_t \partial_{t'} G(t, t')$. We take initial conditions such that $u(0) = 0$, or equivalently $x(0) = 1/2$; the long-time behavior of the correlation function is insensitive to this choice. The closure equation in (5) can then be written as

$$\partial_t \partial_{t'} G(t, t') = \langle f(u(t)) f(u(t')) \rangle. \quad (6)$$

$u(t), u(t')$ are jointly Gaussian with zero means, from which it follows that $1/16 \leq \langle f(u(t)) f(u(t')) \rangle \leq 1$, see App. III. Therefore $tt'/16 < G(t, t') < tt'$, so $\langle u(t)^2 \rangle = G(t, t) \sim t^2$, corresponding to *ballistic* growth of $u(t)$. We show below that $u(t)$ nonetheless repeatedly crosses the origin at arbitrary long times.

The long-time expression for $G(t, t')$ can be worked out from (6). Here we present a different but equivalent derivation, which makes explicit the aging properties of the model. Motivated by the ballistic growth of $u(t)$, we introduce $z(t) \equiv u(t)/t$, and we rescale time though $s \equiv \ln(t)$. The resulting dynamics read

$$z'(s) = -z(s) + \hat{\xi}(s), \quad (7)$$

together with the closure relation (from (5))

$$\langle \hat{\xi}(s) \hat{\xi}(s') \rangle = \langle f(e^s z(s)) f(e^{s'} z(s')) \rangle.$$

Because $z(s)$ is a Gaussian process with finite $O(1)$ variance as $s \rightarrow \infty$, the closure equation becomes in the long-time limit

$$\langle \hat{\xi}(s) \hat{\xi}(s') \rangle = \langle \Theta(z(s)) \Theta(z(s')) \rangle. \quad (8)$$

Equations (7,8) map the original many-body dynamics of (2), in the long-time limit, to chaotic dynamics of random neural networks of the form discussed in [22]. As in [22], at large s , we expect the process in (7) to reach a time-translation invariant chaotic state characterized by

$$\langle \hat{\xi}(s) \hat{\xi}(s') \rangle \equiv \hat{C}(s - s').$$

This corresponds to *aging* of the dynamics in the original time scale $t = e^s$, with correlation time growing linearly with the elapsed time,

$$\lim_{t' \rightarrow \infty} C(t' + \tau, t') = \hat{C}(\ln(1 + \beta)), \quad (9)$$

at fixed $\beta \equiv \tau/t'$. Accordingly, from (7), the $z(s)$ autocorrelation function also admits a time-translation invariant form at large times

$$\langle z(s) z(s') \rangle \equiv \hat{\Delta}(s - s'),$$

which is related to $G(t, t')$ through $\lim_{t' \rightarrow \infty} G(t' + \tau, t')/t'(t' + \tau) = \hat{\Delta}(\ln(1 + \beta))$. We now sketch the derivation of $\hat{\Delta}$. Following [22], $\hat{\Delta}$ and \hat{C} are related by $\hat{C}(s) = -\hat{\Delta}''(s) + \hat{\Delta}(s)$ which, together with (8), implies that $\hat{\Delta}(s)$ satisfies an equation for the motion of a classical particle in a potential V

$$\hat{\Delta}''(s) = -V'(\hat{\Delta}, \Delta_0), \quad (10)$$

where the potential depends parametrically on the initial condition $\Delta_0 \equiv \hat{\Delta}(0)$ and reads,

$$V \equiv -\frac{\hat{\Delta}^2}{2} + \frac{\hat{\Delta}}{4} + \frac{\hat{\Delta}}{2\pi} \left(\sqrt{\frac{\Delta_0^2}{\hat{\Delta}^2} - 1} + \operatorname{arccot} \sqrt{\frac{\Delta_0^2}{\hat{\Delta}^2} - 1} \right).$$

The condition $\hat{\Delta}(s) = \hat{\Delta}(-s)$ implies $\hat{\Delta}'(0) = 0$ so that the $\hat{\Delta}(s)$ trajectory has zero initial kinetic energy. The only physically relevant trajectory is therefore the one converging to the unstable fixed point Δ^* with same potential energy as the initial condition and related to Δ_0 by $V'(\Delta^*, \Delta_0) = 0$ and $V(\Delta^*, \Delta_0) = V(\Delta_0, \Delta_0)$. This gives $\Delta_0 \simeq 0.476$ and $\Delta^* \simeq 0.427$.

The correlation $C(t' + \tau, t') = \frac{1}{S} \sum_i x_i(t' + \tau) x_i(t')$, obtained by running the dynamics (2), is thus expected by (9) to collapse when plotted against τ/t' , as indeed seen in Fig. 1(d), and it matches the correlation function $\hat{C}(s)$ obtained by numerically solving (10) with the appropriate initial conditions. Note that Δ_0 is linked to the long-time mean-square displacement of $u(t)$ as $G(t, t)/t^2 \xrightarrow[t \rightarrow \infty]{} \Delta_0$. Additionally, the auto-correlation satisfies

$$\lim_{t' \rightarrow \infty} C(t', t') = \frac{1}{2} > \lim_{\tau \rightarrow \infty} \lim_{t' \rightarrow \infty} C(t' + \tau, t') = \Delta^*, \quad (11)$$

so that the system continues to evolve, as the correlation with the state at any time is later partially lost. Equation (10) implies a powerlaw relaxation of $C(t, t')$ in the aging regime to its plateau value Δ^* ,

$$\lim_{t' \rightarrow \infty} C(t'(1 + \beta), t') - \Delta^* \underset{\beta \rightarrow \infty}{\sim} \beta^{-k},$$

with $k = \sqrt{|V''(\Delta^*, \Delta_0)|} \simeq 0.492$.

Single variable dynamics—The dynamics (2) pass very close to fixed points at long times. To see this, we calculate the probability distribution of x at time t , $P_t(x)$, taken over many variables in (2), or equivalently over different realizations of (3). Using the fact that $u(t)$ is Gaussian and that $x(t) = f(u(t))$, it reads

$$P_t(x) = \frac{[x(1-x)]^{-1}}{\sqrt{2\pi G(t, t)}} \exp \left[-\frac{1}{2G(t, t)} \left(\ln \frac{x}{1-x} \right)^2 \right]. \quad (12)$$

In particular this implies,

$$\lim_{t \rightarrow \infty} P_t(x) = \frac{1}{2} [\delta(x) + \delta(x-1)]. \quad (13)$$

This shows that the system (2) asymptotically approaches fixed points of the dynamics, where all $x_i \in$

$\{0, 1\}$. Furthermore, at large but finite times, the probability to find $x(t)$ away from the boundaries of $[0, 1]$ decays as $1/t$, with (12) giving

$$\text{Prob}[x(t) \in [\epsilon, 1 - \epsilon]] \underset{t \rightarrow \infty}{\sim} \frac{1}{t} \sqrt{\frac{2}{\pi \Delta_0}} \ln \left(\frac{1 - \epsilon}{\epsilon} \right). \quad (14)$$

for any fixed $\epsilon \in [0, 1/2]$. The probability is thus concentrated exponentially close in time to 0 and 1. Yet the system continues to evolve, see (11), so that none of these fixed points are stable: At long times the system transitions between unstable fixed points, spending ever longer times in their vicinity with fast transitions between them.

In the long-time limit, since $x(s) = \Theta(z(s))$ for $s \rightarrow \infty$, $x(s)$ asymptotically approaches a time-translation invariant two-state process. This is illustrated in Fig. 1(c). Note that as $\Delta^* > 0$ in (11), equation (13) is not the ergodic measure (in log-time) of a single variable $x_i(t)$. In App. IV, we show that for a given degree of freedom the log-time ergodic measure is given by

$$P_{\bar{\xi}}(x) = (1 - p) \delta(x) + p \delta(x - 1), \quad (15)$$

with $p = [1 + \text{Erf}(\bar{\xi}/\sqrt{2\chi})]/2$, where $\bar{\xi}$ is a zero mean Gaussian random variable with variance $\langle \bar{\xi}^2 \rangle = \Delta^*$ and $\chi = \int_0^\infty ds e^{-s} [\hat{C}(s) - \Delta^*]$. So, in a given realization of (2), each variable has an ‘‘identity’’ expressed in the fraction of time (in log-time) it spends near 0 and 1.

Stability of visited fixed points—We found above that at long times the system approaches fixed points, but eventually leaves their vicinity, signaling that they are unstable. We now calculate their entire stability spectrum. The linearized dynamics close to a fixed point \mathbf{x}^* are $\delta x_i = J_{ij} \delta x_j$ with a diagonal matrix $J_{ij} = \delta_{ij} \lambda_i^*$. The growth rates λ_i^* , positive when growing in the direction away from the boundaries, are given by

$$\lambda_i^* = (1 - 2x_i^*) \left(\sum_j \alpha_{ij} x_j^* \right). \quad (16)$$

The stability spectrum of the visited fixed points is therefore equal, at long-times, to the empirical distribution in the many-variable dynamics (2) of $\lambda_i(t) \equiv [1 - 2x_i(t)] \xi_i(t)$ for $i = 1 \dots S$. In the $S \rightarrow \infty$ limit, the stability spectrum is thus equal to the distribution of $\lambda(t) = [1 - 2x(t)] \xi(t)$ in the DMFT framework. It can also be shown that the $\lambda_i(t)$ are independent and identically-distributed random variables, see App. I, therefore the spectrum is self-averaging.

The joint distribution of $\xi(t)$ and $u(t)$ is Gaussian, with correlations $\langle u(t)^2 \rangle = G(t, t)$, $\langle \xi(t)^2 \rangle = C(t, t)$ and cross-correlation $\langle u(t) \xi(t) \rangle$. Changing variables from

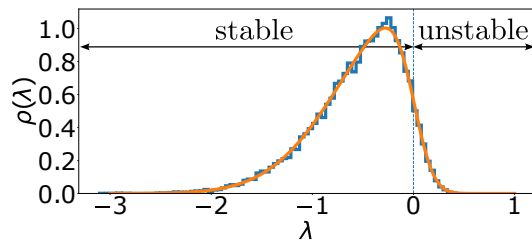


Figure 2. **Stability spectrum of the fixed points visited at long times.** The long-time dynamics evolve in the vicinity of unstable fixed points which all have the same stability spectrum. A finite fraction of the eigenvalues are positive, corresponding to unstable directions around these fixed points. The analytical prediction for the spectrum (17), is in excellent agreement with a simulation (blue) with $S = 2 \cdot 10^4$ variables at $t = 10^8$.

(u, ξ) to (u, λ) and integrating over u , we obtain an expression for the distribution of $\lambda(t)$, reproduced in App. V. Taking its long-time limit, we find that the dynamics (2) transition between fixed points which all have the same stability spectrum

$$\rho(\lambda) = \frac{1}{\sqrt{\pi}} e^{-\lambda^2} \text{Erfc} \left(\frac{\lambda}{\kappa_\infty} \right), \quad (17)$$

with $\kappa_\infty = \sqrt{1/(2\Delta_0) - 1} \simeq 0.224$, see Fig. 2. This distribution has a finite fraction of unstable directions, given by

$$\int_0^\infty \rho(\lambda) d\lambda = \frac{\arctan(\kappa_\infty)}{\pi} \simeq 0.141.$$

This can be compared with the statistics of the full distribution of fixed points of (2). There are 2^S of them and the average number of those with αS unstable directions is given by the binomial law, $\langle \mathcal{N}_\alpha \rangle \sim \exp[Sg(\alpha)]$, with $g(\alpha) = -\alpha \ln \alpha - (1 - \alpha) \ln(1 - \alpha)$. Therefore, in typical fixed points half of the directions are unstable, $\alpha = 1/2$. The dynamics therefore selects in the long-time limit fixed points that are exponentially rare (compared to the typical ones) but that are not the most stable ones existing in the phase space, which are marginal ($\alpha = 0$).

To conclude, we propose an exactly-solvable many-variable model for the dynamics of interacting populations with absorbing boundary values. Its dynamics slow down with a correlation time that grows as the age of the system, see (9). The system evolves in the vicinity of fixed points: In the long-time limit, all variables are found exponentially close in time to absorbing values, see (14). The time it takes for a variable to leave the vicinity of one absorbing value to visit the vicinity of the other is therefore proportional to the age of the system. This explains the scaling of the aging, (9). All these fixed points are unstable, as shown in (17). In the future, it

would be interesting to understand how this scenario is adapted to other many-variable interacting population dynamics, such as the Lotka-Volterra model, where fixed points have degrees of freedom that are not at absorbing values.

-
- [1] Josef Hofbauer and Karl Sigmund. *Evolutionary games and population dynamics*. Cambridge university press, 1998.
- [2] Robert Mac Arthur. Species packing, and zhat competition minimizes. *Proceedings of the National Academy of Sciences*, 64(4):1369–1371, December 1969.
- [3] M Krupa. Robust heteroclinic cycles. page 48.
- [4] Josef Hofbauer. Heteroclinic cycles in ecological differential equations. *Mathematical Institute, Slovak Academy of Sciences*, 1994.
- [5] Robert M. May and Warren J. Leonard. Nonlinear Aspects of Competition Between Three Species. *SIAM Journal on Applied Mathematics*, 29(2):243–253, September 1975.
- [6] Andrea Gaunersdorfer. Time Averages for Heteroclinic Attractors. *SIAM Journal on Applied Mathematics*, 52(5):1476–1489, October 1992.
- [7] F Roy, G Biroli, G Bunin, and C Cammarota. Numerical implementation of dynamical mean field theory for disordered systems: application to the lotka-volterra model of ecosystems. *Journal of Physics A: Mathematical and Theoretical*, 52(48):484001, November 2019.
- [8] Michael T. Pearce, Atish Agarwala, and Daniel S. Fisher. Stabilization of extensive fine-scale diversity by ecologically driven spatiotemporal chaos. *Proceedings of the National Academy of Sciences*, 117(25):14572–14583, June 2020.
- [9] Christoph Ratzke and Jeff Gore. Modifying and reacting to the environmental pH can drive bacterial interactions. *PLOS Biology*, 16(3):e2004248, March 2018.
- [10] Christoph Ratzke, Julien Barrere, and Jeff Gore. Strength of species interactions determines biodiversity and stability in microbial communities. *Nature Ecology & Evolution*, 4(3):376–383, March 2020.
- [11] L. F. Cugliandolo and J. Kurchan. Analytical solution of the off-equilibrium dynamics of a long-range spin-glass model. *Physical Review Letters*, 71(1):173–176, July 1993.
- [12] Jorge Kurchan and Laurent Laloux. Phase space geometry and slow dynamics. *Journal of Physics A: Mathematical and General*, 29(9):1929–1948, May 1996.
- [13] Alessandro Manacorda and Francesco Zamponi. Gradient descent dynamics and the jamming transition in infinite dimensions. *arXiv:2201.01161 [cond-mat]*, January 2022. arXiv: 2201.01161.
- [14] Ada Altieri, Felix Roy, Chiara Cammarota, and Giulio Biroli. Properties of Equilibria and Glassy Phases of the Random Lotka-Volterra Model with Demographic Noise. *Physical Review Letters*, 126(25):258301, June 2021.
- [15] Giulio Biroli, Guy Bunin, and Chiara Cammarota. Marginally stable equilibria in critical ecosystems. *New Journal of Physics*, 20(8):083051, August 2018.
- [16] Leticia F. Cugliandolo, Jorge Kurchan, Pierre Le Doussal, and Luca Peliti. Glassy behaviour in disordered systems with nonrelaxational dynamics. *Physical Review Letters*, 78(2):350–353, January 1997.
- [17] A. Crisanti and H. Sompolinsky. Dynamics of spin systems with randomly asymmetric bonds: Langevin dynamics and a spherical model. *Physical Review A*, 36(10):4922–4939, November 1987.
- [18] Marc Mezard, Giorgio Parisi, and Miguel Angel Virasoro. *Spin Glass Theory And Beyond: An Introduction To The Replica Method And Its Applications*. World Scientific Publishing Company, November 1987.
- [19] H. Sompolinsky and Annette Zippelius. Relaxational dynamics of the Edwards-Anderson model and the mean-field theory of spin-glasses. *Physical Review B*, 25(11):6860–6875, June 1982.
- [20] Chen Liu, Giulio Biroli, David R. Reichman, and Grzegorz Szamel. Dynamics of liquids in the large-dimensional limit. *Physical Review E*, 104(5):054606, November 2021.
- [21] Elisabeth Agoritsas, Giulio Biroli, Pierfrancesco Urbani, and Francesco Zamponi. Out-of-equilibrium dynamical mean-field equations for the perceptron model. *Journal of Physics A: Mathematical and Theoretical*, 51(8):085002, February 2018.
- [22] H. Sompolinsky, A. Crisanti, and H. J. Sommers. Chaos in Random Neural Networks. *Physical Review Letters*, 61(3):259–262, July 1988.
- [23] Florent Krzakala, Federico Ricci-Tersenghi, Lenka Zdeborova, Riccardo Zecchina, Eric W. Tramel, and Leticia F. Cugliandolo. *Statistical Physics, Optimization, Inference, and Message-Passing Algorithms: Lecture Notes of the Les Houches School of Physics: Special Issue, October 2013*. Oxford University Press, December 2015.

Supplemental material for “Aging by near-extinctions in many-variable interacting populations”

I. DYNAMICAL MEAN FIELD THEORY

We derive (3) of the main text, using the cavity method [7, 18]. Consider a system comprised of S degrees of freedom subjected to a perturbation field $h_i(t)$ acting as

$$\dot{x}_i = x_i(1 - x_i) \left(\sum_{j \neq i} \alpha_{ij} x_j + h_i \right).$$

The field $h_i(t)$ serves in the derivation but later set to zero. The linear response function

$$R_{ij}(t, s) = \left. \frac{\delta x_i(t)}{\delta h_j(s)} \right|_{\mathbf{h}=0},$$

obeys

$$\partial_t R_{ij}(t, s) = (1 - 2x_i) \left(\sum_{j \neq i} \alpha_{ij} x_j \right) R_{ij}(t, s) + x_i(1 - x_i) \left(\delta_{ij} \delta(t - s) + \sum_{k \neq i, j} \alpha_{ik} R_{kj}(t, s) + \alpha_{ij} R_{jj}(t, s) \right).$$

From the above equation it follows that $R_{ii}(t, t) = x_i(t) [1 - x_i(t)]$ and $R_{ij}(t, t) = 0$ for $j \neq i$, from which one can deduce the scalings $R_{ii}(t, s) = O(1)$ and $R_{ij}(t, s) = \alpha_{ij} \hat{R}_{ij}(t, s)$ with $\hat{R}_{ij}(t, s) = O(1)$ for $i \neq j$. We can now proceed with the cavity method, by considering a system comprised of $S + 1$ degrees of freedom from which we arbitrarily single out one, labeled x_0 . In the following the indices i, j run from 1 to S . The dynamics of x_0 read

$$\dot{x}_0 = x_0(1 - x_0) \sum_i \alpha_{0i} x_i, \quad (1)$$

and that of the x_i read

$$\dot{x}_i = x_i(1 - x_i) \left(\sum_{j \neq i} \alpha_{ij} x_j + \alpha_{i0} x_0 \right). \quad (2)$$

Therefore a given trajectory of x_0 acts on the x_i as the previously introduced perturbing field \mathbf{h} , when setting $h_i = \alpha_{i0} x_0$. For a given initial condition $x_i(0)$ and a given trajectory $x_0(t)$ we decompose the motion of the $x_i(t)$ as $x_i(t) = x_i^{(0)}(t) + \delta x_i[x_0](t)$ where $x_i^{(0)}(t)$ is the solution of (2) when all the couplings α_{i0} for $i = 1 \dots S$ are set to zero and $\delta x_i[x_0]$ accounts for the correction of the solution due to the dynamics of x_0 . It follows from (1) that describing the dynamics of $x_0(t)$ to $O(1)$ in S only requires to know $\delta x_i[x_0](t)$ up to order $O(1/\sqrt{S})$. We can therefore find δx_i within linear-response, which up to $O(1/S)$ corrections can be written as

$$\delta x_i[x_0](t) = \int_0^t ds \left(R_{ii}(t, s) \alpha_{i0} + \sum_{j \neq i} R_{ij}(t, s) \alpha_{j0} \right) x_0(s).$$

Therefore we have to order $O(1)$,

$$\dot{x}_0 = x_0(1 - x_0) \left[\sum_i \alpha_{0i} x_i^{(0)} + \int_0^t ds \sum_i \alpha_{0i} \left(R_{ii}(t, s) \alpha_{i0} + \sum_{j \neq i} R_{ij}(t, s) \alpha_{j0} \right) x_0(s) \right].$$

Because the interaction matrix is fully asymmetric, $\mathbb{E}[\alpha_{0j}\alpha_{i0}] = 0$, the contribution from the linear response term, $\int_0^t ds..$, scales as $O(1/\sqrt{S})$ and can be neglected. The dynamics of x_0 hence read, up to $O(1/\sqrt{S})$ corrections,

$$\dot{x}_0 = x_0(1 - x_0) \sum_i \alpha_{0i} x_i^{(0)}.$$

We now assume that $x_i^{(0)}$ and $x_j^{(0)}$ (or equivalently x_i and x_j) are weakly correlated processes for $i \neq j$ meaning that for any functional $F[x(t)]$ we have

$$\mathbb{E} \left[\left(F[x_i^{(0)}(t)] - \mathbb{E}[F[x^{(0)}(t)]] \right) \left(F[x_j^{(0)}(t)] - \mathbb{E}[F[x^{(0)}(t)]] \right) \right] \xrightarrow{S \rightarrow \infty} 0, \quad (3)$$

where we have stressed the fact that all variables are statistically identical. Such an assumption, which can be verified self-consistently, is standard in DMFT [23]. It implies a law of large numbers, namely that for any functional $F[x(t)]$

$$\frac{1}{S} \sum_i F[x_i^{(0)}(t)] \xrightarrow{S \rightarrow \infty} \mathbb{E}[F[x^{(0)}(t)]],$$

in agreement with the self-averaging property of the auto-correlation function shown numerically in Fig. 1(d). In the large S limit, $\xi_i \equiv \sum_i \alpha_{0i} x_i^0$ thus converges to a Gaussian process with zero mean and variance

$$\mathbb{E}[\xi_i(t)\xi_i(t')] = \mathbb{E}[x^{(0)}(t)x^{(0)}(t')] = \mathbb{E}[x_0(t)x_0(t')]$$

where we used that, up to order $O(1)$, $x_i^{(0)}$ and x_i and x_0 are statistically identical. This proves (3) of the main text. To see that the weak correlation assumption, (3), is self-consistent within DMFT, we note that the $O(1)$ dynamics of two degrees of freedom x_0 and x_1 read (as the direct interactions between them are only $O(S^{-1/2})$)

$$\dot{x}_0 = x_0(1 - x_0) \sum_{i>1} \alpha_{0i} x_i^{(0,1)},$$

and

$$\dot{x}_1 = x_1(1 - x_1) \sum_{i>1} \alpha_{1i} x_i^{(0,1)},$$

where $x_i^{(0,1)}$ refers to the solution of the many-body dynamics in the absence of both x_0 and x_1 . Upon assuming that (3) holds, the moment generating function of $\xi_0 = \sum_{i>1} \alpha_{0i} x_i^{(0,1)}$ and $\xi_1 = \sum_{i>1} \alpha_{1i} x_i^{(0,1)}$ can be worked out showing that they are independent and identically distributed Gaussian processes. To leading order, the statistical independence of x_0 and x_1 then follows, in agreement with (3). This also implies that the exponential growth rates $\lambda_i(t) \equiv [1 - 2x_i(t)] \xi_i(t)$ in (16) at the dynamically visited fixed points behave, to leading order, as independent and identically distributed random variables in the limit of a large number of degrees of freedom $S \rightarrow \infty$.

II. LOTKA-VOLTERRA SIMULATIONS

In Fig. 1(A), the interaction matrix \mathbf{A} is cyclic with $A_{ii} = 1, A_{i,i+1} = 0.3, A_{i,i-1} = 2$, and all $B_i = 1$. In Fig. 1(B), $S = 2 \cdot 10^4$. The parameters of the Lotka-Volterra dynamics are $B_i = 1$ and an interaction matrix \mathbf{A} defined by $A_{ii} = 1$ and A_{ij} for $i \neq j$ Gaussian variables with mean $\mathbb{E}[A_{ij}] = 10/S$ and variance $\mathbb{E}[A_{ij}A_{kl}] = 2\delta_{ik}\delta_{jl}/\sqrt{S}$.

III. PROOF OF BOUNDS ON $\langle f(u(t))f(u(t')) \rangle$

Here we derive the bounds

$$1/16 \leq \langle f(u(t))f(u(t')) \rangle \leq 1,$$

stated in the main text, below Eq. (6). Indeed, we have first

$$0 < \frac{e^u}{1+e^u} < 1 \Rightarrow \langle f(u(t)) f(u(t')) \rangle < 1.$$

To obtain the lower bound, observe that $u(t)$ and $u(t')$ are jointly Gaussian with correlation matrix

$$M(t, t') = \begin{pmatrix} G(t, t) & G(t, t') \\ G(t, t') & G(t', t') \end{pmatrix}.$$

Therefore

$$\begin{aligned} \langle f(u(t)) f(u(t')) \rangle &> \int_0^{+\infty} \int_0^{+\infty} \frac{du_1}{\sqrt{2\pi}} \frac{du_2}{\sqrt{2\pi}} \frac{\exp(-\frac{1}{2} u^T \cdot M^{-1}(t, t') \cdot u)}{\sqrt{\det M(t, t')}} f(u_1) f(u_2) \\ &> \frac{1}{4} \int_0^{+\infty} \int_0^{+\infty} \frac{du_1}{\sqrt{2\pi}} \frac{du_2}{\sqrt{2\pi}} \frac{\exp(-\frac{1}{2} u^T \cdot M^{-1}(t, t') \cdot u)}{\sqrt{\det M(t, t')}} = \frac{1}{16} \left(1 + \frac{2}{\pi} \operatorname{arccot} \sqrt{\frac{G(t, t)G(t', t')}{G(t, t')^2} - 1} \right) > \frac{1}{16}. \end{aligned}$$

This completes the proof.

IV. ERGODIC MEASURE FOR $x(s)$

We recall (7) of the main text

$$z'(s) = -z(s) + \hat{\xi}(s),$$

and decompose the noise $\hat{\xi}(s)$ as

$$\hat{\xi}(s) = \bar{\xi} + \delta\xi(s)$$

with $\bar{\xi}$ a Gaussian random variable with zero mean and variance $\langle \bar{\xi}^2 \rangle = \Delta^*$ and $\delta\xi(s)$ an independent Gaussian process with zero mean and covariance

$$\langle \delta\xi(s) \delta\xi(s') \rangle = \hat{C}(s, s') - \Delta^*.$$

In the long-time limit, the solution to (7) reads

$$z(s) = \bar{\xi} + e^{-s} \int_0^s ds' e^{-s'} \delta\xi(s'),$$

so that at large s , and fixed $\bar{\xi}$, $z(s)$ is a Gaussian variable with mean $\bar{\xi}$ and variance

$$\langle (z(s) - \bar{\xi})^2 \rangle \xrightarrow{s \rightarrow \infty} \int du e^{-u} [\hat{C}(u) - \Delta^*].$$

Equation (15) of the main text then follows,

$$P_{\bar{\xi}}(x) = (1-p) \delta(x) + p \delta(x-1), \quad (1)$$

with $p = [1 + \operatorname{Erf}(\bar{\xi}/\sqrt{2\chi})]/2$, where $\bar{\xi}$ is a zero mean Gaussian random variable with variance $\langle \bar{\xi}^2 \rangle = \Delta^*$ and $\chi = \int_0^\infty ds e^{-s} [\hat{C}(s) - \Delta^*]$. While each variable switches between 0 and 1 an infinite amount of time, the probability distribution of p (the fraction, in log-time, spent at $x=1$) diverges at 0 (and accordingly at 1) as,

$$P(p) \underset{p \rightarrow 0}{\sim} \left(p \sqrt{-\ln p} \right)^{-1 + \frac{\chi}{\sqrt{\Delta^*}}},$$

with $\chi/\sqrt{\Delta^*} \simeq 0.92$. Namely, some degrees of freedom are strongly biased towards one of the boundaries.

V. STABILITY SPECTRUM

As stated in the main text, the joint distribution of $\xi(t)$ and $u(t)$ is Gaussian,

$$P_t(u, \xi) = \frac{1}{2\pi\sqrt{\det \mathbf{H}}} \exp \left[-\frac{1}{2} (u, \xi) \cdot \mathbf{H}^{-1} \cdot (u, \xi) \right], \quad (1)$$

with the matrix \mathbf{H} given by

$$\mathbf{H} = \begin{pmatrix} G(t, t) & \langle u(t)\xi(t) \rangle \\ \langle u(t)\xi(t) \rangle & C(t, t) \end{pmatrix}.$$

Using this equation, changing variables to (u, λ) and integrating over u , the probability distribution of $\lambda(t)$ is found to be

$$\begin{aligned} \rho_t(\lambda) = & \frac{\sqrt{1+\kappa^2}}{\kappa\sqrt{\pi C(t, t)}} \int_0^{+\infty} \frac{du}{\sqrt{\pi}} \exp \left[-\frac{1+\kappa(t)^2}{2\kappa(t)^2} u^2 - \frac{1+\kappa(t)^2}{2\kappa(t)^2} \frac{\lambda^2}{C(t, t)} \left(\frac{1 - e^{\sqrt{G(t, t)u}}}{1 + e^{\sqrt{G(t, t)u}}} \right)^2 + \frac{\sqrt{1+\kappa(t)^2}}{\kappa(t)^2 \sqrt{C(t, t)}} u \lambda \left(\frac{1 - e^{\sqrt{G(t, t)u}}}{1 + e^{\sqrt{G(t, t)u}}} \right)^2 \right] \\ & \times \left| \frac{1 - e^{\sqrt{G(t, t)u}}}{1 + e^{\sqrt{G(t, t)u}}} \right|, \end{aligned} \quad (2)$$

with

$$\kappa(t) = \sqrt{\frac{C(t, t)G(t, t)}{\langle u(t)\xi(t) \rangle^2} - 1}.$$

At long times,

$$\kappa(t) \rightarrow \kappa_\infty = \lim_{t \rightarrow \infty} \sqrt{\frac{\Delta_0}{2 \left(\int_0^1 C(ts, t) ds \right)^2} - 1} = \sqrt{\frac{1}{2\Delta_0} - 1} \simeq 0.224.$$

where the last equality was obtained by noting that

$$\lim_{t \rightarrow \infty} \int_0^1 C(ts, t) ds = \int_0^{+\infty} ds e^{-s} \hat{C}(s) = \int_0^{+\infty} ds e^{-s} [-\hat{\Delta}''(s) + \hat{\Delta}(s)] = - \int_0^{+\infty} ds \frac{d}{ds} \left\{ e^{-s} [\hat{\Delta}'(s) + \hat{\Delta}(s)] \right\} = \Delta_0.$$

At $t \rightarrow \infty$, equation (2) reduces to (17) of the main text.